Indian Journal of Chemistry
Vol. 59A, January 2020, pp. 21-30

# A novel conductometric titration approach for rapid determination of boron

R Ananthanarayanan[a,*], M P Rajiniganth[a], M Sivaramakrishna[a], B S Panigrahi[b] & B K Panigrahi[a]

[a]Innovative Sensors Section, Security and Innovative Sensors Division, Electronics and Instrumentation Group, Indira Gandhi Centre for Atomic Research, Kalpakkam 603 102, Tamil Nadu, India

[b]Health, Safety and Environment Group, Indira Gandhi Centre for Atomic Research, Kalpakkam 603 102, Tamil Nadu, India

Email: ran1878@igcar.gov.in

*Received 4 January 2019; revised and accepted 20 December 2019*

In laboratories dealing with radioactive samples it is important to minimize both the sample size and also the associated waste generated in an analysis. To meet this objective a rapid conductometric titration technique is developed to determine boron in the moderators of Pressurized Heavy Water Reactors (PHWR's). Using this novel PC interfaced titration facility a minimum tenfold reduction in sample size is achieved compared to conventional conductometric titration. Determination of boron is based on the conversion of extremely weak boric acid to better conducting boron mannitol complex and titrating the complex against NaOH. Various parameters affecting the analysis, when moving from large to small sample size, are analyzed and optimized. The technique is primarily proposed for the assay of boron (≥0.5 ppm) during reactor startup. Each analysis requires less than 10 min. The detection limit is 0.5 ppm and the precision obtained at this level is 4.6% RSD. The technique is a good alternative to less sensitive carminic acid based spectrophotometric method.

**Keywords:** Boron assay, Conductivity detector, Carminic acid method, Pressurized Heavy Water Reactor (PHWR)

Determination of boron is very important due to its wide spread application in glass making, ceramics, health care, food preservation and semi-conductor industries[1–3]. Boron is an important element in nuclear industry because of its high neutron absorption cross section. Natural boron is composed of two isotopes, namely, $B^{10}$ and $B^{11}$ (with 19.8% $B^{10}$ abundance[4]). Neutron poisoning capability of natural boron is derived from $B^{10}$ which has a high thermal neutron absorption cross section of 3840 barns[4]. This particular property makes the presence of boron highly undesirable in nuclear fuels and therefore its estimation is an important quality control parameter during nuclear fuel fabrication[5]. Interestingly, boron and its compounds find significant application in nuclear industry due to its high neutron absorption cross section. $BF_3$ gas filled proportional counters, enriched up to 96% $B^{10}$, are routinely used to detect neutrons[6]. Boron in the form of boron carbide ($B_4C$) is used as control rods in nuclear reactors to manage the neutron flux[7]. Further, boron acts as an effective shielding material[8] for both humans and equipment's against neutrons inside the reactor building. Apart from the above mentioned applications boron is used as a burnable neutron poison in the moderators of PHWR[9]. A few ppm of natural boron, in the form of boron trioxide, is added to the moderator during reactor start up for controlling the reactivity. At this stage the concentration of boron can reach up to a few ppm. To operate the reactor at full power the added boron is slowly removed by passing the moderator through ion exchange beds till its concentration reaches below 30 ppb.

To maintain the reactivity within desired limits during reactor start up, a knowledge on the concentration of boron in the moderator becomes essential for the reactor operator. Therefore, in view of the critical nature of application the analytical technique employed by the quality control laboratory attached to the PHWR should be rapid, accurate and highly precise. There are several sensitive techniques available for trace assay of boron such as inductively coupled plasma mass spectroscopy[9,10,11], high pressure liquid chromatography[12], inductively coupled plasma atomic emission spectroscopy[13], isotopic dilution thermal ionization mass spectrometry[4,9,14] and ion chromatography (IC)[5,15]. For analyzing moderator samples collected during reactor operation, when the expected boron concentration is <30 ppb, IC is preferred among the above mentioned techniques. However, these techniques are not employed during reactor start up when the boron concentration is at

ppm levels. Generally, such sensitive techniques are reserved for trace analysis as they are time consuming. Kilroy *et.al.*, has reported an atomic absorption spectroscopic method (AAS)[16] to determine boron. AAS using graphite furnace suffers from low sensitivity and poor reproducibility due to the formation of refractory carbides in the graphite tube[17]. Further, the technique is susceptible to severe matrix interference. Boron has been estimated by neutron activation analysis (NAA) techniques[18–20] as well. Techniques based on NAA are practically not feasible for routine and rapid analysis as the samples need to be first irradiated with neutrons in a nuclear reactor before its actual analysis. Generally, pH titration and spectrophotometric techniques are employed for assaying boron in the moderator samples collected during the reactor startup. Although pH titration[21] is simple as it requires large sample volumes (50–100 mL) for analysis. With regard to spectrophotometric technique, two different approaches, viz., carminic acid[22] and curcumin[23,24] based methods are used. From rapidity point of view both the techniques are equally time consuming. However, the former is relatively simple but less sensitive while the latter is laborious but highly sensitive. Earlier, one of the authors had reported the assay of boron by conductometric titration approach[25] which also suffers from the drawback of a higher sample requirement. This technique requires 50 mL of sample for analysis at sub-ppm levels. Our earlier work primarily focused on understanding the nature of titration plots in isotopically different aqueous mediums, namely, light water and heavy water and also to understand the effect of interfering and non interfering impurities during analysis.

In the present work attention is directed towards reducing the sample volume required to assay boron in the heavy water moderators of PHWR during the reactor startup by conductometric titration approach. In radioactive laboratories by reducing the sample size the dose received by the analyst and the active waste generated after analysis is reduced. Therefore, the current work assumes significance from radioactive point of view. The titration facility needed to achieve tenfold reduction in sample volume as compared to conventional titration and a specially designed high performing flow through conductivity detector, which forms the heart of the experimental set up, are described in detail. The various parameters that affect the analysis, as one moves from large to small sample size, and their optimization is also discussed. In particular, the effect of conversion of excess hydroxide aliquots to bicarbonate, which takes place during the course of titration and its impact on the analysis, is dealt in detail. The proposed technique is validated against two other independent techniques. Finally, the method has been successfully applied to determine boron in the moderators of Madras Atomic Power Station (MAPS) during the reactor start up.

## Materials and Methods

### Chemical reagents

All the chemicals used in this work were of AR grade. Reactor grade heavy water with isotopic purity of 99.75% (w/w), as established by infrared spectroscopy, was obtained from MAPS. Heavy water was used to prepare boron stock solution as well as the working standards while Millipore water with conductivity <1 μS $cm^{-1}$ was used to prepare NaOH and $NaHCO_3$ solutions. Boron stock solution (~2000 mg $L^{-1}$) was prepared by dissolving ~0.18 g of $B_2O_3$ in 25 mL of heavy water. $B_2O_3$ dissolves in $D_2O$ to give $B(OD)_3$[$B_2O_3 + 3D_2O \rightarrow 2\ B(OD)_3$]. The solution was standardized against freshly prepared 0.1 N sodium hydroxide using phenolphthalein indicator and was stored in a plastic volumetric flask.

### Experimental Setup

For carrying out conductometric titrations with small sample volumes (2.5–5.0 mL) an innovative titration facility, entirely fabricated and assembled in-house, was used. Each analysis requires 2.5 mL of sample. However, larger sample volumes can be taken for analysis. The block diagram of the experimental facility is shown in Fig. 1 while the photograph of the titration facility is shown in Fig. 2. The setup consists of a small titration vessel, an in-house made low cell volume (~3 μL) conductivity detector, a miniperistaltic pump to circulate the contents of the titration vessel through the detector during titration, a signal routing unit to transmit the signals generated from the detector to the PC, a PC loaded with a graphical user interface (GUI) to record the titration plots, a magnetic stirrer and a magnetic bar to bring the contents of the titration vessel to a homogeneous mixture during the titration.

### Digital Instrumentation

For reliably capturing extremely small shifts in conductivity occurring in less sensitive $D_2O$ medium,

an in-house developed detector working entirely in digital domain was used. Since the first electronic response of such a conductivity measuring device is directly in digital domain it offers a host of advantages such as; simplified instrumentation due to elimination of signal conditioner, analog to digital converters, pre amplifiers and post amplifiers that are normally associated with conventional instruments, low power consumption as the probe is powered by 5 V DC, excellent noise immunity, long distance signal transmission and ready compatibility of digital signals with PC.

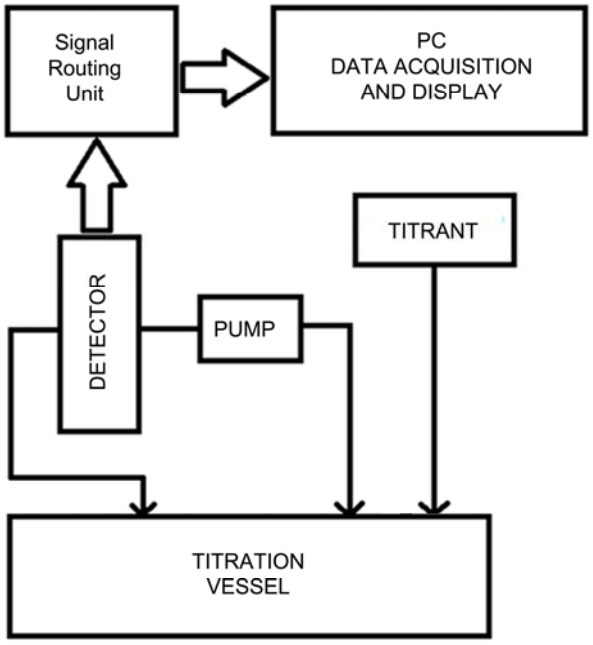


Fig. 1 — Block diagram of the experimental setup to carry out conductometric titrations with small sample volumes.

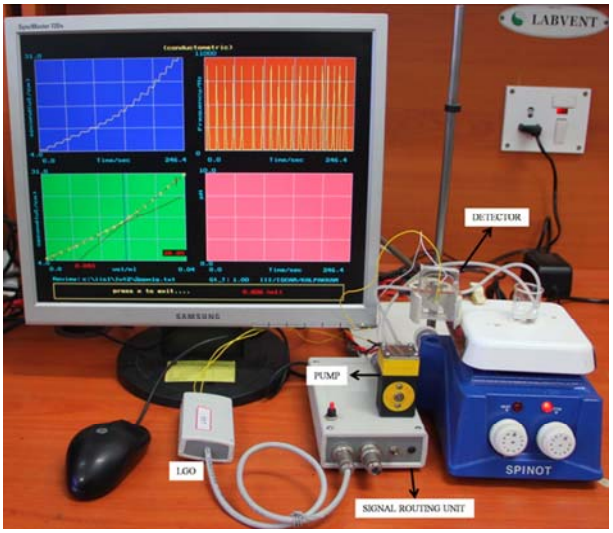


Fig. 2 — Photograph of the titration facility.

The schematic diagram of the resistance capacitance (RC) type logic gate oscillator (LGO) circuit used in this work is shown in Fig. 3. A 1 nF capacitor and the low cell volume conductivity probe (refer 3.1) constitute the fixed C part and the variable R part of the LGO circuit respectively. The output of the LGO oscillates between 0 V and 5 V and therefore producing a train of rectangular digital pulses. Using a signal routing cum power supply unit the digital pulses are transmitted to the PC. Frequency, defined as the number of pulses per unit time, is solely a function of solution conductivity as sensed by the electrodes of the conductivity probe. Or in other words frequency carries information on the prevailing conductivity of the solution. Through suitable calibration a quantitative relationship is established between frequency and conductivity. Procedure to calibrate the conductivity detector, detailed instrumentation, typical applications of digital conductivity meters are described in detail elsewhere[26,27,28].

**Graphical User Interface (GUI)**

The GUI used in the present work has been developed in-house and is coded in C language. Some of the salient features of the GUI are: (i) receiving digital pulses from the signal routing unit, (ii) counting the pulses for fixed duration to determine the frequency, (iii) computing the solution conductivity from the frequency value, (v) displaying the titration plot in real time during analysis, (v) unfolding the plot in volume domain immediately after titration, (vi) detecting titration end point and (vii) saving the data for future use.

During titration the GUI plots, the solution conductivity is a function of real time. This particular

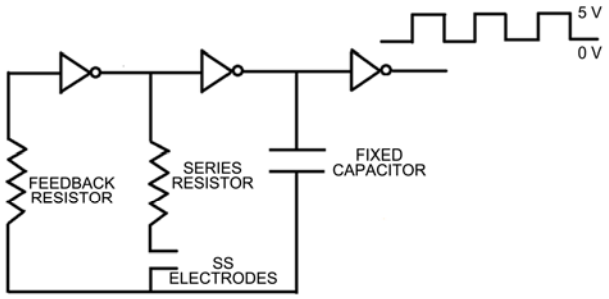


Fig. 3 — Schematic diagram of the LGO circuit. A pair of circular stainless steel electrodes constitutes the variable resistance part of the circuit.

feature of capturing data in real time serves as a useful tool for carrying out kinetic studies. In the course of titration, before each addition of titrant aliquot a momentary electronic signal is communicated from the signal routing unit to the GUI. These signals essentially serve as a time marker to identify the individual aliquots. By knowing the volume corresponding to a titrant aliquot and the conductivity value prevailing just prior to the addition of each aliquot (as indicated by time marker) the GUI constructs the volume domain plot. The plot appears immediately after the titration along with the real time plot for further analysis.

**Methodology**

Sample of 4 mL boron was introduced into the reaction vessel and purged with argon for about 3 min to expel the dissolved carbon dioxide. Appropriate quantity of solid mannitol was added to make the sample 2% with respect to mannitol. To carry out titration the contents of the reaction vessel was circulated through the conductivity detector and the titrant was delivered manually using a gas tight Hamilton syringe. Flow of inert gas inside the titration vessel was uninterrupted throughout the titration. After analysis, volume of titrant consumed by boron mannitol complex was accurately determined using the GUI by the intersection of least square fitted lines of adjacent slopes. From the resulting stoichiometric end point boron present in the sample was quantified.

## Results and Discussion

**Innovative titration setup**

For measuring sample conductivity (k) the probe geometry decides the minimum volume of the sample. Modern probes in general require 25–50 mL of sample owing to their large cell volumes. This is also true for now popular four electrode probes that avoid errors caused by polarization effect[29]. Therefore, to circumvent high sample requirement a flow type probe having a cell volume of ~3 µL is integrated into the titration set up. The schematic diagram of the in-house made low cell volume conductivity probe is shown in Fig. 4a, while its photograph is presented in Fig. 4b. The probe was fabricated with high precision using computer numerical controlled lathe machine. A pair of circular stainless steel electrodes of 3 mm diameter placed opposite to each other in close proximity (0.5 mm) and perpendicular to the direction of flow of liquid constitute the sensing electrodes. Fluctuations in conductivity, caused by stray air bubbles trapped in the sample, are completely eliminated in our design as the flow path is free from obstruction. This is not the case with a particular type of design reported earlier[30]. Here, two thin Pt wires that act as sensing electrodes are placed closely to each other inside the tube carrying the sample. Although easy to construct, in this configuration a high probability exists for the air bubble to get trapped between the electrodes or in between an electrode and the wall of the tube.

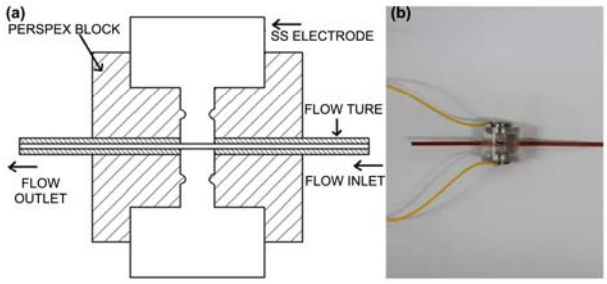


Fig. 4 — (a) Schematic diagram of the assembled conductivity probe and (b) photograph of the low cell volume conductivity probe.

With our modified design the cell volume and therefore the sample size required for measuring k is drastically reduced to few µL (~3 µL). However, such flow through type detectors, typically used to detect eluted ions from IC columns, require an external module to bring the probing medium in contact with the sensing electrodes. In the proposed technique a small peristaltic pump serves the purpose well. If a compact pump is absent a lab made unit is realized with a small stepper motor, driver circuit, rollers and a frame to hold the motor. To analyze beta active moderator samples the titration facility must be compact in order to reduce its foot print inside the fume hood. Towards this objective a small peristaltic pump and miniaturized instrumentation were used. With the modified titration set up each analysis requires only 2.5 mL, a 10 fold reduction in sample volume as compared to conventional titrations.

**Scoping studies**

To quantify boron use of certain polyhydroxy alcohols such as mannitol, sorbitol and glycerol is well known[31,32]. For the present study mannitol was used. Boron mannitol complex in $D_2O$ for the sake of brevity is represented as DX. Here, $D^+$ and $X^-$ refer to deuterium cation and bulky anion part respectively. A typical DX vs NaOH plot in heavy water by conventional titration approach (Fig. 5), viz., by taking 25 mL of sample and using a dip type probe while the governing reaction is presented as equation 1.

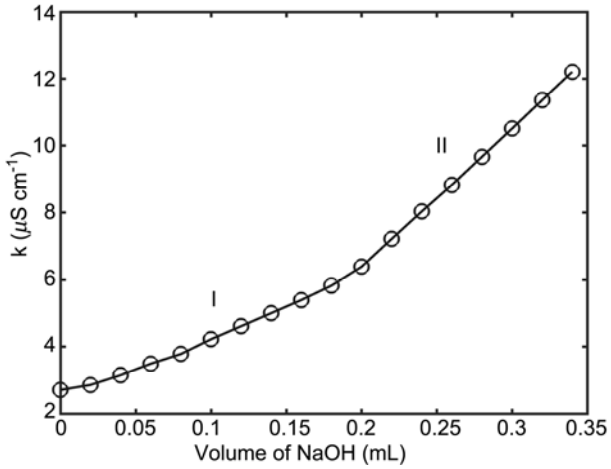


Fig. 5 — A conventional titration plot obtained by taking 25 mL of sample and using a dip type probe (1 ppm of boron complexed with mannitol titrated against 0.011 N NaOH in 20 μL steps; end point 0.2 mL corresponding to 0.95 ppm of boron).

$$DX + NaOH \rightarrow NaX + DOH \quad ...(1)$$

Influence of $D_2O$ matrix on conductivity measurements, role of mannitol and manifestation of regions I and II (refer Fig. 5) are discussed in detail elsewhere[25]. Henceforth, in further discussions regions I and II will refer to the two characteristic regions of DX vs NaOH plot. Although DX is relatively stronger than boric acid still it is a weak acid (pKa = 4.1) and therefore its accurate quantification at sub ppm levels poses a challenge. Moreover, the problem is small sample size and estimation in a less sensitive $D_2O$ medium compounds. Therefore, in the first phase feasibility studies with small sample volumes and the various parameters influencing the analysis were investigated in detail. It is to be noted that, all titrations were carried in $D_2O$ medium and at no point light water was used. Further, unless specifically stated all the titrations were carried out by purging argon to the sample before titration (~3 min) also during the titration.

We observed that sample size, titrant strength and the constant time interval (Δt) existing between the addition of successive titrant aliquots during titration influenced the analysis. B estimation with sample volumes ≥4 mL gave well demarcated end point. However, the end point was diffused, especially at lower boron concentrations, when the sample size was reduced further. Since the aim was to minimize the radioactive waste generated after analysis and replace carminic acid technique, which is employed when expected boron concentration is ≥ 2 ppm during reactor start up, a sample volume of 4 mL was chosen for subsequent studies. With regard to titrant strength optimization studies were carried out by taking 0.01 N, 0.025 N and 0.05 N NaOH. In all the three cases, irrespective of titrant strength, the plots showed two distinct regions (I and II). Finally, to investigate the role of Δt on analysis titrations were carried out by varying Δt from 10 s to 100 s. A lower limit of 10 s was arrived based on the mixing time, i.e., time required to homogenize the solution after addition of a titrant aliquot. The mixing time was experimentally determined to be ~8.5 s. Δt was found to exert a major influence on the resulting plot profile. As Δt increased the slope of region II approached that of region I. Eventually, at large Δt's (≥50 s) the slopes became equal and the resulting plot appeared as a single straight line. In other words no end point was detected when using large Δt's.

The detailed results obtained from the scoping studies is given in Table 1. Referring to Table 1 one can arrive at the following conclusions, (i) recovery up to 0.5 ppm of B is feasible with 4 mL of sample volume, (ii) under similar conditions better accuracy and precision is obtained with 0.05 N NaOH (refer samp. no 5–10), (iii) at a B level of 0.5 ppm recovery is possible only using a Δt of 10 s (refer samp. no 11–13) and (iv) in general, compared to large Δt's, smaller Δt's produce better results (refer samp. no 11–16).

Besides the three parameters discussed above the nature of titrant was also investigated. It is obvious that as the difference between the slopes of region I and II increases so does the sensitivity of the technique. Hence, one must select conditions that favor an enhanced difference between the slopes. One such potential parameter is based on nature of titrant. $K^+$ due to its higher equivalent conductance ($\lambda_o$=73.5 S cm$^2$ eq$^{-1}$)[33] is more conducting then $Na^+$ ($\lambda_o$=50.11 S cm$^2$ eq$^{-1}$)[33], since, k and $\lambda_o$ are related by the well known equation $k= \lambda_o C$. As $OH^-$ is common, KOH is expected to impart a greater positive slope to region II as compared to NaOH. However, no perceptible improvement in plots was observed by replacing NaOH with KOH. Hence, it is concluded that either NaOH or KOH can actas titrants.

**Analysis of real time titration plot**

As stated earlier after the analysis there is a provision to analyze volume domain as well as real time plots. Careful inspection of real time plots obtained at various Δt's revealed an interesting

Table 1 — Results obtained from the scoping study

| Samp. No | Boron added/ mg $L^{-1}$ | Boron recovered by the current technique/ mg $L^{-1}$ | Parameters influencing titration plot | | |
|---|---|---|---|---|---|
| | | | Sample volume/mL | Δt/ S | Titrant strength/ N |
| 1 | 1.0 | Not detected | 2.5 | 10 | 0.05 |
| 2 | 1.0 | Not detected | 3.0 | 10 | 0.05 |
| 3 | 1.0 | 1.23±0.09 (n=3) | 4.0 | 10 | 0.05 |
| 4 | 1.0 | 1.15±0.09 (n=3) | 5.0 | 10 | 0.05 |
| 5 | 0.55 | 0.78±0.03 (n=4) | 4.0 | 10 | 0.01 |
| 6 | 0.55 | 0.79±0.03 (n=4) | 4.0 | 10 | 0.025 |
| 7 | 0.55 | 0.72±0.03 (n=4) | 4.0 | 10 | 0.05 |
| 8 | 1.4 | 1.55±0.08 (n=4) | 4.0 | 10 | 0.01 |
| 9 | 1.4 | 1.58±0.07 (n=4) | 4.0 | 10 | 0.025 |
| 10 | 1.4 | 1.53±0.08 (n=4) | 4.0 | 10 | 0.05 |
| 11 | 0.5 | 0.63±0.05 (n=3) | 4.0 | 10 | 0.05 |
| 12 | 0.5 | Not detected | 4.0 | 25 | 0.05 |
| 13 | 0.5 | Not detected | 4.0 | 100 | 0.05 |
| 14 | 1.0 | 1.09±0.09 (n=3) | 4.0 | 10 | 0.05 |
| 15 | 1.0 | 1.45±0.10 (n=3) | 4.0 | 25 | 0.05 |
| 16 | 1.0 | Not detected | 4.0 | 75 | 0.05 |

phenomenon. As an example, the observation is illustrated with Fig. 6, which shows a time domain plot obtained at 0.5 ppm B using a Δt of 100 s. The plot is partitioned into pre end point and post end point regions, designated as R1 and R2 respectively. In the plot several spikes are encountered at regular intervals. The spikes represent the transient state after each aliquot addition and prior to homogenization of the physico chemical system under investigation. Spikes in R1 and R2 are derived from two different sources in accordance with Eqn 1. In R1 spikes are formed due to accumulation of $Na^+$ $X^-$ ion pair whereas spikes in R2 are caused by the accumulation of excess titrant ions, i.e., $Na^+$ and $OH^-$. On careful examination one finds flat and stable plateaus in R1 whereas unstable plateaus in R2. For clarity, a flat and an unstable plateau are zoomed out and presented as inset figures in their respective regions. Flat plateaus reflect systems stability and in R1 chemical inertness of $Na^+$ $X^-$ brings in the stability. However in R2, unlike in R1, after the initial rise a steady decrease in conductivity is observed. One can attribute such an observation to the time dependent dynamic changes occurring inside the reaction vessel. In this particular case instability can be attributed to conversion of excess hydroxide aliquots to bicarbonate according to equations 2 and 3.

$$2NaOH + CO_2\,(aq) \rightarrow Na_2CO_3 + H_2O \quad \ldots (2)$$

$$Na_2CO_3 + CO_2\,(aq) + H_2O \rightarrow 2NaHCO_3 \quad \ldots (3)$$

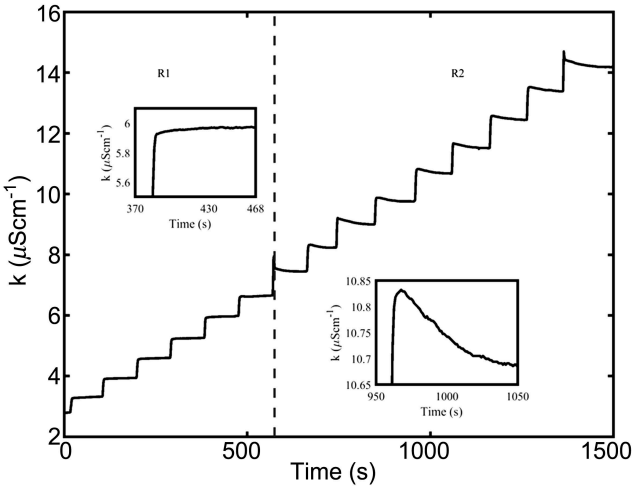


Fig. 6 — Real time titration plot of 0.5 ppm boron pre-treated with mannitol against 0.05 N NaOH obtained using a Δt of 100 s. Inset figures show the zoomed in view of a small portion of the plot in the pre end point (R1) and post end point regions (R2), respectively.

$OH^-$ is converted to $HCO_3^-$ via the intermediary $CO_3^{2-}$, which is formed by the reaction of free $OH^-$ with dissolved $CO_2$ present inside the titration vessel. The $\lambda_o$ of $HCO_3^-$ and $OH^-$ are 44.5 S $cm^2$ $eq^{-1}$ and 199.2 S $cm^2$ $eq^{-1}$, respectively[33]. Therefore, under similar conditions of concentration and temperature, $HCO_3^-$ contributes far less to solution conductivity than $OH^-$. In conclusion, replacement of $OH^-$ with $HCO_3^-$ causes the solution conductivity to decrease as reflected in inset of R2 in Fig. 6.

**Validation of $OH^-$ - $HCO_3^-$ conversion**

Conversion of excess hydroxide aliquots, added post the end point, to bicarbonate is assumed to proceed according to Eqns 2 and 3. Therefore, the assumption needs experimental validation. One can in principle validate the conversion, if dilute NaOH and $NaHCO_3$ solutions are separately titrated against HCl and the plots are compared. In case of conversion plots will be identical. To validate, dilute NaOH and $NaHCO_3$ solutions, each containing $2.5\times10^{-5}$ M of respective anions, were titrated against 0.1 N HCl. During assay of B the overall $OH^-$ strength, due to addition of a titrant aliquot after the end point, typically is in the order of $\sim10^{-5}$ M. Hence, a representative concentration of $2.5\times10^{-5}$ M was chosen. Since interference from atmospheric $CO_2$ is suspected titrations were performed without purging argon inside the sample. The plots obtained due to NaOH vs HCl and $NaHCO_3$ vs HCl are compared in Fig. 7 and are represented as 1 and 2 respectively. Because the plots are identical uptake of atmospheric $CO_2$ and subsequent conversion of $OH^-$ to $HCO_3^-$ is established. Further, for the sake of ready reference the typical profile of NaOH vs HCl plot is presented as inset of Fig. 7.

Conditions employed in the validation discussed above fail to mimic the real scenario, since in B assay titrations are carried out by flushing argon in to the sample. Presence of argon avoids the interference from carbonic acid, a very weak acid generated due to the dissolution of atmospheric carbon dioxide into the sample. Carbonic acid introduces positive error in analysis as it consumes a small portion of the titrant. Hence, to complete the proof $OH^-$ vs HCl and $HCO_3^-$ vs HCl titrations discussed above were repeated in presence of argon. The resulting superimposed plots, not presented here to avoid repetition, also resembled the plots shown in Fig. 7 and thus completing the proof.

It is interesting to note that, in spite of flushing argon inside the sample during titration (also before the start of titration), $OH^-$ is converted to $HCO_3^-$. This indicates a minor ingress of atmospheric $CO_2$ into the sample. To probe this aspect further a series of dilute NaOH solutions ranging from $10^{-4}$ M to $10^{-5}$ M were titrated against HCl in presence of argon. The extent of conversion of NaOH, expressed in terms of percentage, as a function of initial strength of NaOH taken for titration (Fig. 8). As evident from the figure, conversion increases as concentration of NaOH decreases. Complete conversion occurs at 0.1 mM and

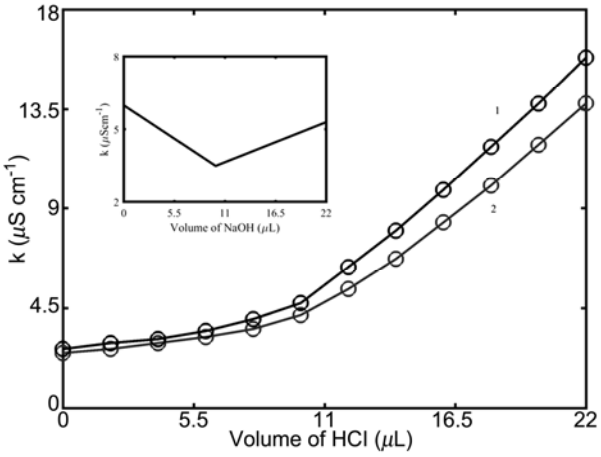


Fig. 7 — Comparison of plots obtained by titrating (a) 4 mL of $2.5\times10^{-5}$M NaOH against 0.01 N HCl in 2.0 µL steps and (b) 4.0 mL of $2.5\times10^{-5}$ M $NaHCO_3$ against 0.01 N HCl in 2.0 µL steps. Inset shows the typical profile of the NaOH Vs HCl plot.

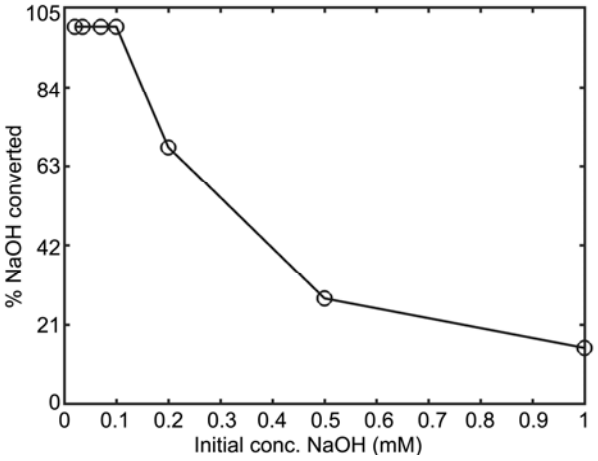


Fig. 8 — Fraction of NaOH converted (in terms of %) as a function of initial concentration of NaOH taken for titration.

further dilutions. It is also inferred that at low concentrations (≤0.1 mM) presence of argon probably delays the conversion but not its complete arrest.

**Consequence of $OH^-$ - $HCO_3^-$ conversion**

During B determination we observed that, Δt not only governs the extent of formation of $HCO_3^-$ from excess $OH^-$ aliquots but also the resulting plot profile. To illustrate this point, a plot obtained with Δt=10 s and another with Δt=100 s, and representing two extreme cases, are compared in Fig. 9 (plot 9 (a)) and inset of Fig. 9 (plot 9 (b)), respectively. Plot 9(b) appears as a single straight line while plot 9(a) shows two distinct slopes (dk/dv) that are delineated by a dashed vertical line. This observation can be rationalized as follows. As described earlier (ref 2.4), by picking select data from real time plot the GUI

unfolds the corresponding volume domain plot. Due to the use of a large Δt in case of plot 9(b), highly conducting $OH^-$ ions are converted to poorly conducting $HCO_3^-$ ions at every addition of aliquot post the end point. Therefore, for constructing region II GUI picks significantly lower k values. This is not the case with plot 9(a). Here, excess $OH^-$ aliquots are not consumed due to quick addition of successive aliquots. As a result, the values constituting region II of plot 9(a) are much higher than those of region II of plot 9(b). Consequently, in plot 9(a) regions I and II are well demarcated while they are indistinguishable in plot 9(b). For intermediate Δt values between 10 and 100 s, as expected the resulting slope (region II) falls in between those of plots 9(a) and 9(b). It should be noted that, irrespective of Δt the slope of region I remained the same. This is because, in the pre end point region of corresponding real time plots conductivity values are almost stable across each plateau. In conclusion, for unambiguous demarcation of end point and to improve the limit of detection and accuracy, two key figures of merit in analysis, quick addition of titrant becomes a prerequisite. A conclusion that is consistent with the results obtained from the scoping studies (refer Table 1).

**Titrations with optimized parameters**

To accurately delineate regions I and II, a detailed evaluation of various parameters leads to the following optimized conditions; Δt should be 10 s, minimum sample volume should be 4 mL, titrant strength must be 0.05 N and either KOH or NaOH can serve as titrant. Under the optimized conditions

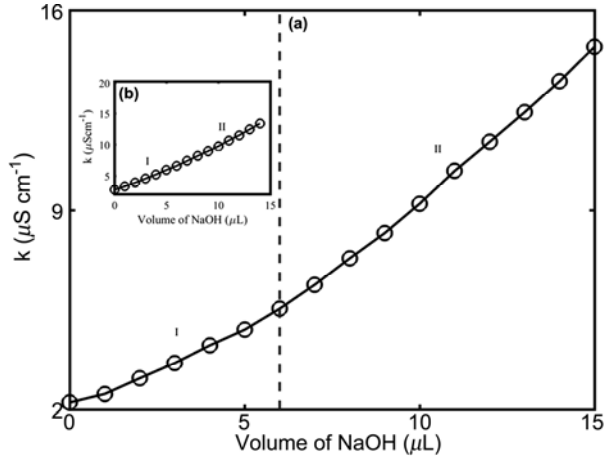


Fig. 9 — Typical titration plot of 0.5 ppm boron complexed mannitol against 0.05 N NaOH using a Δt of 10 s. Inset shows the same plot obtained using a Δt of 100 s.

several experimental runs were carried out with spiked samples. A typical plot generated at a B level of 2.1 ppm is shown in Fig. 10. It can be seen that end point can be detected through visual inspection. This feature clearly demonstrates that, by reducing the sample size by a factor of six as compared to conventional titration, the quality of plot is not compromised. Although demarcation through visual inspection is possible, to improve accuracy and precision, the end point was always determined using the GUI (inset Fig. 10).

**Method validation**

We validated the proposed technique against two independent techniques, viz., (i) carminic acid spectrophotometric technique and (ii) conventional conductometric titration approach by taking 25 or 50 mL sample volume. All absorbance measurements were carried out at 590 nm using a Thermo make 2600 UV-visible spectrophotometer equipped with a 10 mm path length cell. For the second approach, a dip type pulsating type conductivity probe was employed.

Carminic acid forms a reddish blue complex with boron in concentrated sulphuric acid medium. The color intensity of the complex reaches a maximum in ~30 min. A typical spectral scan of boron-carminic acid complex is presented in Fig. 11. The scan shows a fairly stable plateau from 580 to 630 nm. Hence, absorbance measurements were carried out at 590 nm. The results obtained from all the three independent

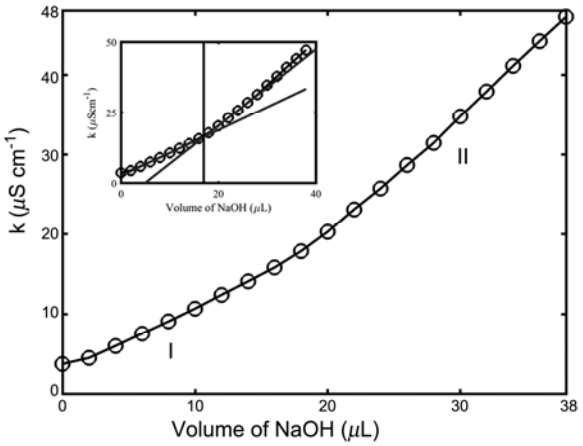


Fig. 10 — A typical titration plot obtained using optimized parameters (4 mL sample containing 2.1 ppm boron pretreated with mannitol was titrated against 0.05 N NaOH in 2 µL steps). Inset figure shows the exact determination of end point by the intersection of least square fitted lines of regions I and II; end point corresponds to a boron concentration of 2.2 ppm as against 2.1 ppm.

Table 2 — Comparison of present technique with carminic acid spectrophotometric approach and conventional conductometric titration approach

| Sample No[a,b,c] | Boron added/ mg $L^{-1}$ | Boron assayed by the current technique/ mg $L^{-1}$ | Boron recovered by specrophotometric technique/ mg $L^{-1}$ | Boron recovered by conventional conductometric titration technique/ mg $L^{-1}$ |
|---|---|---|---|---|
| 1 | 4.3 | 4.24±0.25 | 4.18±0.24 | 4.25±0.14 |
| 2 | 2.25 | 2.41±0.08 | 2.43±0.27 | 2.29±0.06 |
| 3 | 1.8 | 1.89±0.07 | 1.99±0.29 | 1.74±0.05 |
| 4 | 3.0 | 3.10±0.11 | 3.26±0.23 | 3.10±0.08 |
| 5 | 0.5 | 0.65±0.03 | - | 0.56±0.03 |
| 6 | - | 1.92±0.07 | - | 1.78±0.05 |
| 7 | - | 1.30±0.06 | - | 1.21±0.03 |
| 8 | - | 0.92±0.05 | - | 0.85±0.03 |
| 9 | - | 1.72±0.05 | - | 1.65±0.04 |

[a]Samples 1 to 5 correspond to spiked samples while samples 6 to 9 correspond to actual moderator samples taken during reactor start up.
[b]n=4 for spiked samples and n=3 for moderator samples.
[c]25mL of sample was taken for all the analysis carried out by conventional conductometric titration technique except sample number 5. For sample number 5, 50 mL was taken for analysis.

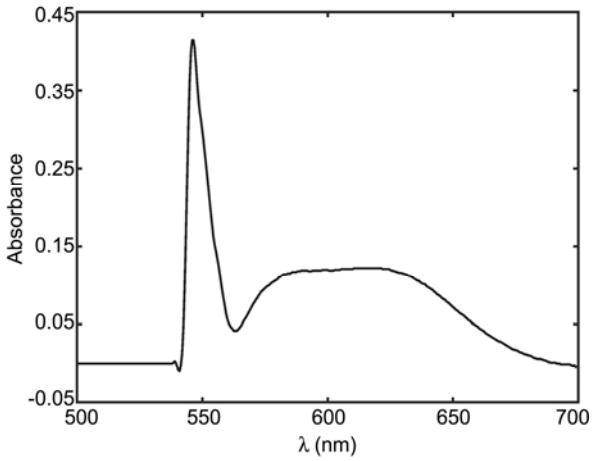


Fig. 11 — Spectral scan of boron mannitol complex using a 10 mm pathlength cell.

techniques are compared in Table 2. Among the three techniques carminic acid approach is least precise. Also, the technique is most time consuming and least convenient. In addition to the above shortcomings, the use of concentrated sulfuric acid introduces a potential safety hazard. The proposed technique and the conventional conductometric titration technique compare well in terms of precision, rapidity and convenience. However, unlike the latter technique the former method reduces the sample waste by a factor of six. The precision of the current technique in the entire range of interest (0.5–4 ppm) falls between 2.9% to 5.89 % RSD. The technique was further deployed to assay boron in the moderator samples of MAPS reactor collected during reactor start up. For analyzing moderator samples, the current technique and conventional conductometric titration approaches were only employed. Necessary precautions while handling moderator samples, including carrying out analysis inside the fume hood, were followed. The results of the analysis are also presented in Table 2 and the results agree with the conventional conductometric titration technique. Hence, the proposed technique proves to be attractive and convenient for assaying B in the moderators of PHWR during the reactor startup. Finally, to fully automate the analysis work is being carried out to fabricate and integrate a volume dispenser with the existing titration facility. This will not only improve the overall precision in analysis, by eliminating errors associated with manual addition, but also the overall convenience especially when dealing with large number of samples.

## Conclusions

A novel conductometric titration technique is developed for boron determination in the moderator circuit of PHWR's by taking significantly reduced sample size. Probably, for the first time a low cell volume conductivity probe is used in a titration to reduce the sample volume. The study clearly demonstrates the optimization of various parameters required to detect boron unambiguously using a sample volume of 4 mL and in a less sensitive $D_2O$ matrix. Compared to other techniques (carminic acid, curcumin and pH titration techniques) that are followed to determine boron during reactor start up, the proposed technique is simple, rapid and generates minimum radioactive waste. Especially, compared to carminic acid technique, the present technique

achieves lower detection limit and is relatively safe as it avoids use of concentrated sulphuric acid. The proposed titration facility is not limited to assay of boron but can be readily adopted to quantify other chemical species when there is a need to reduce the sample size as in the case with active laboratories.

**Acknowledgement**

The authors thank Dr. Hari Krishna, MAPS for providing different batches of heavy water samples. They are thankful to Shri Manogaran and Smt Thulasi for their experimental support and to Smt Malathi and Shri Chitrakumar for their instrumentation support.

**References**

1 Sah R N & Brown P H, *Microchem J*, 56 (1997) 285.
2 Kumar S D, Maiti B & Mathur P K, *Anal Chem*, 71 (1999) 2551.
3 Melnyk M, Goncharuk V, Butnyk I & Tsapiuk E, *Desalination*, 185 (2005) 147
4 Rein J E & Abernathey R M, *Talanta*, 19 (1972) 857.
5 Jeyakumar S, Raut V V & Ramakumar K L, *Talanta*, 76 (2008) 1246.
6 Knoll G F, *Radiation detection and measurement*, (John Wiley & sons, New York) 507.
7 Steinbruck M, *J Nucl Mater*, 336 (2005) 185.
8 Cacuci D G, *Handbook of nuclear engineering vol 1*, (Springer, Germany), 2010 p. 1428.
9 Aggarwal S K & You C F, *Mass Spectrom Rev*, 36 (2017) 499.
10 Sun D H, Ma R L, Mc Leod C W, Wang X R & Cox A G, *J Anal At Spectrom*, 15 (2000) 257.
11 Gregoire D C, *J Anal At Spectrom*, 5 (1990) 623.
12 Rao R M & Aggarwal S K, *Talanta*, 75 (2008) 585.
13 Ball J W, Thomson J M & Jenne A E, *Anal Chim Acta*, 98 (1978) 67.
14 Rao R M, Parab A R, Bhusan K S & Aggarwal S K, *Mikrochim Acta*, 169 (2010) 227.
15 Tapparo, Pastore P & Bombi G G, *Analyst*, 123 (1998) 1771.
16 Kilroy W P & Moynihan C T, *Anal Chim Acta*, 83 (1976) 389.
17 Matusaki K, Yamaguchi T & Yamamoto Y, *Anal Sci*, 12 (1996) 301.
18 Isenhour T L & Morrison G H, *Anal Chem*, 38 (1966) 167.
19 Acharya R, *J Radioanal Nucl Chem*, 281 (2009) 291.
20 Ramanjaneyulu P S, Sayi Y S, Nathaniel T N, Reddy A V R & Ramakumar K L, *J Radioanal Nucl Chem*, 273 (2007) 411.
21 Silverman L & Bradshaw W, *Anal Chim Acta*, 12 (1955) 177.
22 Callicoat D L & Wolszon J D, *Anal Chem*, 31 (1959) 1434.
23 Grotheer E W, *Anal Chem*, 51 (1979) 2402.
24 Spicer G S & Slickland J D H, *Anal Chem Acta*, 18 (1958) 231.
25 Ananthanarayanan R, Sahoo P & Murali N, *Indian J Chem Technol*, 19 (2012) 278.
26 Sahoo P, Ananthanarayanan R, Malathi N, Rajiniganth M P, Murali N & Swaminathan P, *Anal Chim Acta*, 669 (2010) 17.
27 Ananthanarayanan R, Sahoo P & Murali N, *J Radioanal Nucl Chem*, 299 (2014) 293.
28 Sahoo P, Malathi N, Praveen K, Ananthanarayanan R, Arun A D, Murali N & Swaminathan P, *Rev Sci Instrum*, 81 (2010) 1.
29 Reinhardt K & Kern W, *Handbook of silicon water cleaning technology*, (Elsevier, Cambridge) 2018, p.647.
30 Dasgupta P K & L Bao, *Anal Chem*, 65 (1993) 1003.
31 Geffen N, Semiat R, Eisen M S, Balazs Y, Katz I & Dosoretz C G, *J Membr Sci*, 286, (2006) 45.
32 Vogel A I, *A text book of qualitative inorganic analysis*, (John Wiley & Sons, New York) 1961, p.253
33 Dean J A, *Lange's handbook of chemistry*, (McGraw Hill, New York) 1992, p.8.159.